American Mineralogist, Volume 69, pages 754–770, 1984

Crystal structure and cation distribution in titanomagnetites ($Fe_{3-x}Ti_xO_4$)

Barry A. Wechsler,[1] Donald H. Lindsley, and Charles T. Prewitt

Department of Earth and Space Sciences
State University of New York
Stony Brook, New York 11794

Abstract

A systematic study of the crystal structure of titanomagnetites was undertaken to characterize the effects of composition and quenching temperature on the cation distribution. Powder specimens ranging in composition from pure magnetite to a slightly nonstoichiometric ulvöspinel were synthesized at temperatures between 930 and 1350°C. Several specimens quenched from 1350°C were later annealed at 800°C for up to 95 days. Unit-cell parameters were determined by X-ray diffraction, and saturation magnetization values were measured at room temperature on a vibrating sample magnetometer. The oxygen coordinate, thermal parameters, and sublattice magnetizations were determined from neutron diffraction data using profile refinement techniques.

No significant differences were found in the unit-cell parameters or magnetization resulting from different synthesis temperatures or annealing, and no change was observed in the oxygen positional parameters following annealing. Ti occupies only octahedral sites in all specimens. Temperature factors increase markedly with Ti content, indicating static positional disorder due to mixing of Fe and Ti on octahedral sites. Values of the saturation magnetization and individual sublattice magnetic moments are consistent with the cation distribution model of Akimoto and do not support models that propose a quenchable, temperature-dependent Fe^{2+}–Fe^{3+} distribution. Diffuse scattering in the neutron diffraction patterns suggests the presence of short-range order, possibly involving octahedral cations, but no long-range order inconsistent with space group $Fd3m$ was found. Systematic trends in the oxygen position and unit-cell parameter as a function of composition may be influenced by octahedral cation interactions.

Introduction

Minerals in the solid solution series between magnetite (Fe_3O_4) and ulvöspinel (Fe_2TiO_4) are common constituents of a wide variety of igneous and metamorphic rocks. Intermediate members of the series, referred to here as titanomagnetites, are the primary carriers of rock magnetism and, as such, have been the subject of numerous experimental and theoretical investigations. The magnetic properties of these materials are critically dependent upon their composition, degree of oxidation and intracrystalline cation distribution, and thus may be affected not only by conditions during petrogenesis, but by their subsequent thermal history as well.

Recent studies of deep-sea basalts have stimulated a great deal of interest in titanomagnetites and their oxidized equivalents, the titanomaghemites (e.g., Readman and O'Reilly, 1972; Keefer and Shive, 1981; Moskowitz and Banerjee, 1981). When found in rocks coexisting with a hematite–ilmenite solid solution, the titanomagnetites may also be useful as indicators of the temperature and oxygen fugacity under which these phases equilibrated (Lindsley, 1963; Buddington and Lindsley, 1964). In recent years, attempts have been made to model the thermochemistry of these solid solutions (Rumble, 1970, 1977; Powell and Powell, 1977; Lindsley, 1978; Spencer and Lindsley, 1981). A major stumbling block to the success of these efforts has been the lack of understanding of the equilibrium cation distribution. The resulting uncertainty in the configurational entropy, which produces free energy uncertainties on the order of several kcal/mole at 1000°C, is a significant factor in solution models and cannot be neglected.

Thus, the crystal structure and cation distribution in titanomagnetites are of interest both for their importance in determining the magnetic properties of these minerals and because of the need to account accurately for their thermochemical behavior. Although a number of previous studies have examined this system, their results have been somewhat conflicting and incomplete. The present study attempts to resolve some of the discrepancies by

[1] Present address: Hughes Research Laboratories, 3011 Malibu Canyon Road, Malibu, California 90265.

0003–004X/84/0708–0754$02.00

combining X-ray and neutron diffraction techniques with magnetic measurements on synthetic specimens given a variety of heat treatments.

Previous studies

Both magnetite and ulvöspinel have the inverse spinel structure, with space group *Fd3m* (Bragg, 1915a,b; Nishikawa, 1915; Barth and Posnjak, 1932). This structure incorporates one tetrahedrally-coordinated cation and two octahedrally-coordinated cations per four oxygens. In end-member magnetite, the Fe^{2+} is all octahedral, whereas Fe^{3+} is distributed over both tetrahedral and octahedral sites. In ulvöspinel all the Ti is octahedral and Fe^{2+} occupies both tetrahedral and octahedral sites. The distribution of the species Fe^{2+}, Fe^{3+}, and Ti^{4+} between the tetrahedral (A) sites and octahedral (B) sites for intermediate compositions, however, is uncertain. Several studies have suggested the possibility that at least some Ti may exist in the tetrahedral site (Gorter, 1957; Forster and Hall, 1965; Stout and Bayliss, 1980); however, other magnetic measurements (O'Reilly and Banerjee, 1965; Stephenson, 1969) and neutron diffraction studies (Ishikawa et al., 1964, 1971) are best explained if Ti^{4+} is always limited to the octahedral site.

A number of models have been proposed for the distribution of Fe^{2+} and Fe^{3+} in the solid solution series, based largely upon the results of magnetic measurements of natural and synthetic specimens. Akimoto (1954) suggested a simple substitution model in which the occupancy of each site varies linearly between the two end-member compositions. Assuming colinear ferrimagnetic ordering (Néel, 1948), the saturation magnetization for such a model would also be linearly dependent upon composition.

Néel (1955) and Chevallier et al. (1955) proposed a model based upon expected crystal-chemical preferences, in which Fe^{2+} always prefers octahedral coordination and Fe^{3+} always prefers tetrahedral coordination. Such a substitution scheme is discontinuous, and would produce a trend in saturation magnetization and other properties with a break at $x = 0.5$ (where x represents mole fraction Fe_2TiO_4). An intermediate model (O'Reilly and Banerjee, 1965) follows the Néel substitution from $x = 0$ to $x = 0.2$ and from $x = 0.8$ to $x = 1.0$, while following an Akimoto-type substitution scheme in between, producing saturation magnetization values lower than the Akimoto model, but higher than the Néel model, for $x = 0.2$ to $x = 0.8$.

Stephenson (1969) and Bleil (1971, 1976) have proposed a temperature-dependent distribution of Fe^{2+} and Fe^{3+} to explain the apparent variation of saturation magnetization for samples quenched from different temperatures. These models give the Akimoto distribution as the equilibrium configuration for high temperatures (essentially 1300°C to the melting point) and suggest the Néel model as the equilibrium configuration for low temperatures. For intermediate temperatures, the cation distribution would be continuously variable.

There are a number of difficulties with these models, however. The Akimoto model requires that Fe^{3+} (A) = Fe^{3+} (B) and Fe^{2+} (B) = 1.0 per formula unit throughout. These requirements are suggestive of symmetry constraints that would be inconsistent with the *Fd3m* space group and might require lower symmetry than the low-temperature distribution models. Furthermore, the Akimoto model is in some sense an arbitrary high-temperature limit, because a statistically random distribution of Fe^{2+} and Fe^{3+} would give a higher configurational entropy and might therefore be preferred at high temperatures. The O'Reilly–Banerjee distribution is similarly disconcerting in that it proposes two discontinuities in the cation substitution scheme without clear evidence for a causative mechanism.

These models have assumed that end-member magnetite retains the inverse spinel structure at high temperatures. However, diffusion studies on magnetite (Flood and Hill, 1957; Dieckmann and Schmalzried, 1977) suggest a random cation distribution at high temperature. Mössbauer spectra of magnetite above the Curie temperature (Evans, 1973, 1975; van der Woude et al., 1968) also suggest the disappearance of discrete Fe^{2+} and Fe^{3+} species, with all Fe species closely approaching the +3 oxidation state. Recent thermoelectric measurements (Mason and Bowen, 1981; Wu and Mason, 1981) also support the suggestion of a statistically random cation distribution in magnetite at high temperature.

The Curie temperature and unit-cell parameters of titanomagnetites should be dependent upon the cation distribution (Prevot and Poix, 1971; Stephenson, 1972), and should, therefore, reflect the thermal history, if the cation distribution is sensitive to temperature. However, previous studies have failed to demonstrate such a dependence.

A further argument against the temperature-dependent models was suggested by Jensen and Shive (1973), who proposed that it was impossible to quench in a high-temperature cation distribution since re-equilibration requires only the transfer of an electron between adjacent tetrahedral and octahedral sites. The energy difference between A- and B-site Fe is too small, in their view, to inhibit rapid electron transfer.

These models have also been based primarily upon magnetization measurements, and inferences about the cation distribution require assumptions of the magnitude and orientation of ionic magnetic moments in the structure. Thus, data on the individual site moments are essential to confirm these observations.

Finally, all of the magnetization measurements were performed on different suites of quenched specimens, but the investigators advocating a temperature dependence never attempted to demonstrate that the cation distribution of a given specimen could be re-equilibrated by annealing at temperatures either above or below the

initial quenching temperature. Recently, however, O'Donovan and O'Reilly (1980) reported such an experiment. Specimens of synthetic Mg-bearing titanomagnetites, originally quenched from 1350 and 1425°C, were annealed at 600 and 1000°C for up to 5 hours. No change was found in the saturation magnetization, Curie temperature, or unit-cell parameters after annealing.

Fujino (1974) performed X-ray structure refinements of single-crystal titanomagnetites grown from the melt and powder samples prepared by sintering at 1000°C in evacuated silica tubes. He concluded that there was a significant difference in the trends of A–O and B–O distances with composition for the two suites of specimens, in support of the hypothesis of a temperature-dependent Fe^{2+}–Fe^{3+} distribution. However, given the reported uncertainties in Fujino's measurements and the limited number of data, this conclusion may not be justified. The data presented in this paper are in general agreement with Fujino's results but provide a more sensitive test on this question due to greater precision in the diffraction experiments.

Some phase equilibria results do suggest the possibility of a temperature effect on the cation distribution in titanomagnetites. Experimental phase composition data of coexisting titanomagnetites and hematite-ilmenites (Buddington and Lindsley, 1964; Spencer and Lindsley, 1981) under a variety of oxygen buffers and hydrothermal conditions, show a change in slope at about 850°C. This feature might reflect a change in cation ordering over a fairly narrow temperature interval in the titanomagnetite phase.

Experimental procedures

Synthesis of samples

All samples used in this study were synthesized from mixes of high-purity Fe_2O_3, TiO_2, and Fe sponge. Stoichiometric mixes were prepared by first mixing Fe_2O_3 and TiO_2 in the desired proportions. These were ground in an automatic agate mortar under ethanol for 2–3 hours. Finally, Fe sponge was added to the mix, after which grinding continued for an additional hour.

Specimens with compositions between 0 and 80 mole % Fe_2TiO_4 were prepared by sintering in Ag-foil lined, evacuated SiO_2-glass tubes. Run times at 930°C varied from 4 to 7 days, after which the capsules were opened and run products were examined optically and by X-ray diffraction. For compositions with $x > 0.3$, it was considered desirable to react the charges further to improve sample homogeneity. These samples were ground for ~1 hour in the agate mortar and were then wrapped in Ag foil and reloaded into SiO_2-glass capsules and reacted for an additional 5 to 6 days. See Table 1 for synthesis conditions of all samples.

A different method was used to prepare high-temperature specimens for neutron diffraction and magnetic studies. Compositions with 0, 25, 50, and 75 mole % Fe_2TiO_4 were prepared in a two-stage sintering process involving a low-temperature "prereaction" stage followed by grinding and further reaction at high temperature in a vertical furnace with a controlled H_2–CO_2 gas mixture at a total pressure of 1 atm. The mixes were first placed in a Ag-foil crucible and reacted at about 900°C for 15 minutes in a CO–CO_2 gas mixture chosen to produce no weight change during reaction. X-ray diffraction patterns showed the material after this first sintering to be composed of a single phase spinel for the pure magnetite composition, and a multi-phase assemblage of two spinels, wüstite, ilmenite, and rutile for Ti-bearing compositions. The products were then ground in an agate mortar for 1 hr. Pellets were formed by pressing this material into the bottom of a 12 mm I.D. SiO_2-glass tube which was then evacuated and sintered at ~800°C for 15–20 mins. The sintered pellet was removed from the tube and suspended in the vertical furnace from a 0.004 inch Pt wire which extended through the center of the pellet.

Phase equilibrium data on the Fe–Ti–O system (Webster and Bright, 1961; Taylor, 1964; Katsura et al., 1976; Simons and Woermann, 1978) suggest that deviations from Fe_3O_4–Fe_2TiO_4 stoichiometry in the spinel phase are primarily in the direction of oxygen-rich, cation-deficient compositions at high temperatures. Relatively little, if any, solubility of wüstite in the spinel has been found. Therefore, in order to minimize vacancies and produce an essentially stoichiometric spinel, the oxygen fugacity was maintained at values appropriate to wüstite saturation. Gas mixtures for each composition were chosen in a series of experiments with small pellets in which the H_2/CO_2 ratio was adjusted in steps of 0.01–0.02 log units fO_2 to determine the boundary between the spinel and spinel + wüstite fields. Presence of wüstite was determined from X-ray diffraction patterns, with an estimated detection limit of ≤0.5 wt.%.

Due to the large sample requirements of the powder neutron diffraction technique (sample holder volume ≃ 4 cm^3), it was necessary to synthesize the material for each composition in a number of separate batches. From 4 to 6 batches of 4 to 5 grams each were run to produce the desired amount of material. H_2 and CO_2 were monitored with separate flowmeters, and a total volume of 8 ml/sec, corresponding to a linear flow rate of 0.7 cm/sec, was maintained for all syntheses. Use of a solid-electrolyte fO_2 sensor (Sato, 1971; Williams, 1972) during early stages of the synthesis experiments confirmed the stability of the gas mixing ratio during the course of a run, as well as the values of fO_2 calculated from the H_2–CO_2 ratios using the values of Deines et al. (1974). Run times at 1350°C were 4 hours, which was found to be more than sufficient to ensure optical and X-ray homogeneity. At the end of 4 hours, the pellets were dropped onto a pool of Hg at the bottom of the furnace tube, still in the same atmosphere. The pellets broke into many fragments and cooled to below incandescent temperatures throughout within 5–10 seconds. Of course, much of the exposed surface area cooled more quickly than this. Run products from each batch were first X-rayed separately, to ensure homogeneity, and all batches were then combined to form a composite specimen.

X-ray diffraction patterns of all specimens revealed a single phase spinel with sharp peaks. In the USP25, USP50, and USP75 specimens, a trace of wüstite was present, with an estimated abundance of ≤1–2 wt.%. Reflected light microscopy revealed small grains of wüstite (1–5 μm in diameter) dispersed throughout the spinel grains in at least one of the specimens, suggesting the wüstite formed in equilibrium with spinel during reaction at 1350°C.

Recent experiments by Simons and Woermann (1978) indicate that near the ulvöspinel end of the Fe_3O_4–Fe_2TiO_4 solid solution series, stoichiometric spinel is unstable relative to the assemblage metallic Fe + cation-deficient spinel. Their results also

Table 1. Synthesis conditions

ID	Nominal Comp'n. (Mole % Fe_2TiO_4)	Starting Material	Capsule	Atm	-log fO_2	T(°C)	Time
MT100-1350	0	$Fe+Fe_2O_3$	P	H_2+CO_2	6.97	1350	4h
USP25-1350	25	$Fe+Fe_2O_3+TiO_2$	P	H_2+CO_2	7.34	1350	4h
USP50-1350	50	$Fe+Fe_2O_3+TiO_2$	P	H_2+CO_2	7.98	1350	4h
USP75-1350	75	$Fe+Fe_2O_3+TiO_2$	P	H_2+CO_2	8.97	1350	4h
USP100-1200	"100"†	$Fe+FeO_{1+x}+TiO_2$	Fe foil, evac SiO_2			1200	18h
MT100-1350,800A	0	MT100-1350	evac SiO_2			800	28d 22h
USP25-1350,800A	25	USP25-1350	Ag foil, evac SiO_2			800	95d 2h
USP50-1350,800A	50	USP50-1350	Ag foil, evac SiO_2			800	70d 18h
USP75-1350,800A	75	USP75-1350	Ag foil, evac SiO_2			800	57d 15h
MT100-930	0	$Fe+Fe_2O_3$	Ag foil, evac SiO_2			930	5d
USP10-930	10	$Fe+Fe_2O_3+TiO_2$	Ag foil, evac SiO_2			930	5d 3h
USP20-930	20	$Fe+Fe_2O_3+TiO_2$	Ag foil, evac SiO_2			930	4d 1h
USP30-930	30	$Fe+Fe_2O_3+TiO_2$	Ag foil, evac SiO_2			930	5d 3h
USP40-930	40	$Fe+Fe_2O_3+TiO_2$	Ag foil, evac SiO_2			930	12d 16h*
USP60-930	60	$Fe+Fe_2O_3+TiO_2$	Ag foil, evac SiO_2			930	12d 16h*
USP70-930	70	$Fe+Fe_2O_3+TiO_2$	Ag foil, evac SiO_2			930	10d 22h*
USP72.5-930	72.5	$Fe+Fe_2O_3+TiO_2$	Ag foil, evac SiO_2			930	10d 22h*
USP75-930	75	$Fe+Fe_2O_3+TiO_2$	Ag foil, evac SiO_2			930	10d 22h*
USP77.5-930	77.5	$Fe+Fe_2O_3+TiO_2$	Ag foil, evac SiO_2			930	10d 22h*
USP80-930	80	$Fe+Fe_2O_3+TiO_2$	Ag foil, evac SiO_2			930	9d 22h*

P indicates sample pelletized, suspended in gas mixture, total pressure = 1 atm.
** indicates intermediate grinding.*
† *Nominal formula:* $Fe_{1.933}Ti_{1.035}\square_{0.032}O_4$.

suggest that a single-phase spinel on the FeO–TiO_2 join, containing neither Fe^{3+} nor Ti^{3+}, is stable in equilibrium with metallic Fe and ilmenite at ~1200°C with $FeO/(FeO+TiO_2) \cong 0.65$. Reconnaissance experiments with compositions varying from $FeO/(FeO+TiO_2) = 0.64$ to 0.666 (i.e., stoichiometric Fe_2TiO_4) at temperatures ranging from 930 to 1220°C were consistent with these findings.

The sample of USP100 was therefore synthesized by reacting a mix of composition $FeO/(FeO+TiO_2) = 0.651$ (molar) wrapped in Fe foil in evacuated SiO_2-glass tubes at 1200°C. Run times were 18 hours, and the synthesis was done in 6 separate batches of 3–4 grams each. During reaction at 1200°C, several of the capsules developed minor leaks, allowing penetration of air into the charges and resulting in weight gains of a few mg. However, it is believed that all excess oxygen was absorbed by the outer surfaces of the Fe foil (inner surfaces were not tarnished) and that the run products were unaffected by this leakage. Optical, X-ray, and magnetic examination revealed no differences between the material from capsules with and without leakage. X-ray diffraction patterns of the composite specimen showed a well-crystallized spinel phase and a small amount (≤2 wt.%) of ilmenite.

Following collection of the initial neutron diffraction data, three specimens (USP25, USP50, USP75) were annealed at 800°C for 57–95 days. Each specimen was divided into three batches and loaded into Ag-lined silica tubes which were then evacuated, dried, and sealed. The tubes were placed in a horizontal furnace and held at 800±5°C. After annealing, each batch was checked by X-ray diffraction before they were recombined to form a composite sample. No wüstite could be detected in any of the samples following the annealing.

Neutron diffraction data collection

Neutron diffraction powder patterns were obtained on a three-axis spectrometer at the High Flux Beam Reactor at Brookhaven National Laboratory. Samples were held in a 1 cm diameter cylindrical vanadium holder. Neutron wavelengths of ~1.3Å were selected using a Ge monochromator in the (111) diffracting condition, and the diffracted beam was passed through a pyrolitic graphite analyzing crystal with the (004) plane in diffracting position. 20-min Soller slits were installed before and after the monochromator and between the sample and analyzer. 40-min slits were used between the analyzer and BF_3 detector. Step widths were 0.05 degree two-theta with the exception of USP50-1350, for which a 0.1 degree step width was used. Counting times were of the order of 1–4 min per step. Incident beam intensity was monitored with a fission counter to ensure equal incident beam intensity for each step. Scans were made in the range two-

Table 3. Final positional parameters, isotropic temperature factors (Å^2), and magnetic moments (μ_B)

	u	B_A	B_B	B_{ox}	μ^A_{Fe}	μ^B_{Fe}	R_I	R_p	R_p(wt)
MT100-1350	0.25470(18)	0.37(4)	0.47(4)	0.64(5)	4.01(5)	3.70(3)	1.00	4.82	6.66
USP25-1350	0.25519(21)	0.46(4)	0.51(4)	0.62(4)	3.81(8)	3.51(6)	2.21	8.17	11.23
USP25-1350,800A	0.25520(10)	0.46(2)	0.41(2)	0.65(2)	3.71(4)	3.54(3)	1.11	5.18	6.46
USP50-1350	0.25702(19)	0.58(4)	0.43(5)	0.73(4)	3.12(10)	3.00(9)	2.53	7.68	9.56
USP50-1350 (77 K)	0.25654(22)	0.43(7)	0.13(11)	0.57(6)	3.92(7)	3.73(6)	1.04	4.43	6.04
USP50-1350,800A	0.25704(11)	0.64(2)	0.55(3)	0.85(2)	3.06(6)	2.99(6)	1.36	8.33	9.96
USP75-1350	0.25919(9)	0.67(2)	0.57(3)	0.94(3)*			2.44	6.94	8.65
USP75-1350,800A	0.25912(6)	0.75(2)	0.60(2)	1.06(3)*			1.67	6.61	7.77
USP100-1200	0.26038(7)	0.84(2)	0.64(4)	1.34(3)*			1.59	5.53	6.51

*Equivalent isotropic B.
Results refer to room temperature except where indicated.
Numbers in parentheses refer to estimated standard deviation in least significant units.
Space group Fd3m; A site at 1/8, 1/8, 1/8; B site at 1/2, 1/2, 1/2; Oxygen at u, u, u.
(Coordinates referred to origin at center of symmetry.)
μ^A_{Fe} and μ^B_{Fe} refer to the magnetic moments per Fe atom on the A and B sites, respectively.
$R_I = 100\ \Sigma|I(obs)-(1/c)I(calc)|/\Sigma I(obs)$.
$R_p = 100\ \Sigma|y(obs)-(1/c)y(calc)|/\Sigma y(obs)$.
$R_p(wt) = 100(\Sigma W[y(obs)-(1/c)y(calc)]^2/\Sigma W[y(obs)]^2)^{1/2}$

theta = 13–110° ($\sin\Theta/\lambda < 0.65$). The raw profile intensity data are listed in Table 2.[2]

The sample of USP50-1350 was also studied at 77 K. For this experiment the sample was loaded into an aluminum sample holder in a He atmosphere. The sample cup was placed in an aluminum dewar which was evacuated and cooled with liquid nitrogen during data collection.

Refinement procedures

Structure refinements were carried out using the profile refinement method of Rietveld (1969) and the computer programs as modified by Hewat (1973) and Khattak and Cox (1977). The background intensity was determined by averaging over 10–20 steps every few degrees, or less often at higher angles, where background is infrequently reached. The neutron scattering lengths for Fe, Ti, and O were 0.95, −0.34, and 0.58. Form factors for the magnetic ions were taken from Watson and Freeman (1961). Profile parameters varied were the two-theta zero-point, three half-width parameters, and unit-cell parameter. Structural parameters varied were scale factor, oxygen positional parameter, temperature factors for each site, and magnetic moments of Fe on the A and B sites. Final results are reported in Table 3, and selected interatomic distances and angles are given in Table 4.

In early refinements, an average Fe^{2+}–Fe^{3+} form factor was used for all Fe atoms, since it was not possible to determine both the Fe^{2+}–Fe^{3+} occupancies and magnetic moments independently. However, it was later found that use of a pure Fe^{3+} form factor significantly improved the refinements. Final refinements, therefore, used this form factor. This may indicate a slight "contraction" of the valence electrons of Fe in the spinel crystals relative to the free ion state for which the form factors were calculated.

For the annealed specimens, it was also found advantageous to exclude the 440 reflection from the refinements. This was the most intense peak in the patterns and was found to give consistently large negative values of I_{obs}–I_{calc}, possibly because of extinction. However, it was included in all refinements of unannealed specimens. The 111 peaks were also excluded from both the annealed and unannealed specimens of USP75. This peak was very diffuse in these data sets, perhaps the result of critical magnetic scattering. The Curie temperature for the titanomagnetite series reaches room temperature close to the composition x = 0.75 (Akimoto et al., 1957; Bleil, 1976). However, the actual Curie temperature of USP75 was not determined.

Table 4. Selected interatomic distances (Å) and angles (°)

	MT100-1350	USP25-1350,800A	USP50-1350,800A	USP75-1350,800A	USP100-1200
A-O	1.886(3)	1.900(2)	1.935(2)	1.976(1)	2.001(1)
B-O	2.060(2)	2.063(1)	2.058(1)	2.052(1)	2.049(1)
A-A	3.6355(1)	3.6475(1)	3.6645(1)	3.6835(1)	3.6957(1)
B-B	2.9684(1)	2.9782(1)	2.9920(1)	3.0076(1)	3.0175(1)
A-B	3.4807(1)	3.4922(1)	3.5085(1)	3.5267(1)	3.5384(1)
O-O (tet)	3.080(4)	3.102(2)	3.161(3)	3.227(2)	3.268(2)
O-O (oct)*	2.9694(1)	2.9795(1)	2.9944(1)	3.0116(1)	3.0227(1)
O-O (oct)**	2.857(4)	2.854(2)	2.824(3)	2.788(2)	2.767(2)
O-B-O	87.78(9)	87.54(5)	86.64(5)	85.59(3)	84.94(4)
O-B-O	92.22(9)	92.46(5)	93.36(5)	94.41(3)	95.06(4)
$OAV^{\dagger}$	5.4	6.6	12.3	21.2	27.9
$QE^{\dagger\dagger}$	1.0015	1.0018	1.0033	1.0057	1.0074

*Unshared edge.
**Shared edge.
†Octahedral angle variance (°^{2}).
††Quadratic elongation.

[2] To receive a copy of Table 2, order Document AM-84-249 from the Business Office, Mineralogical Society of America, 2000 Florida Avenue, N.W., Washington, D. C. 20009. Please remit $5.00 in advance for the microfiche.

Large values of isotropic temperature factors and relatively high *R*-indices in early refinements of the USP75 and USP100 specimens suggested the possibility that static positional disorder resulting from mixing of Fe and Ti on the octahedral sites might be contributing to the apparent thermal factors. In order to account for this, anisotropic thermal ellipsoids were refined for the oxygen atoms in USP75-1350, USP75-1350,800A and USP100-1200, which led to significant improvements in these refinements. Values of the rms displacements for these atoms are given in Table 5. The octahedral sites were not found to be significantly anisotropic. Anisotropic temperature factors were also allowed to vary for the other data sets but did not result in any improvements of the fits or in any significant anisotropic oxygen ellipsoids. Therefore, only isotropic B's were varied in final refinements.

The usefulness of the profile refinement method, and in particular the accuracy of estimated parameter errors using this technique, has been challenged by Sakata and Cooper (1980). However, Prince (1981) suggests that for well-resolved, uncomplicated patterns that are adequately fit by the structure model, the errors are not likely to be seriously underestimated. In order to evaluate this problem, several data sets were also refined using integrated intensities with the program MOWLS (D. E. Cox, pers. comm.). This program allows overlapping peaks to be considered as a single observation.

Parameters refined in this way were in all cases within one esd of the values determined from the profile method. The parameter errors derived from the integrated intensity refinements were generally within 1 to 1.25 times those obtained with the profile method. Thus, it is concluded that the profile refinement method was satisfactory and the reported esd's are not significantly underestimated. The profile refinement method was preferred, however, because of its inherently greater ability to make use of the regions of overlapping peaks at high angles.

Magnetic measurements

Hysteresis loops and saturation magnetization values at room temperature were measured on a vibrating sample magnetometer at the NASA Goddard Space Flight Center. The instrument was calibrated before data collection with a Ni standard of known magnetization. Powder samples weighing 0.04–0.06 gm were held in plastic sample cups. Fields up to ±20,000 oersteds were employed to saturate the samples. Saturation moments were determined by extrapolating the magnetization curves to infinite applied field (H) using the relation $M = M_S(1\text{-}a/H)$. Constricted loops were found for samples with 50–80 mole % Fe_2TiO_4. Small amounts of ferro- or ferrimagnetic impurities were also found to be present in specimens with $x \geq 0.75$. This is consistent with the presence of metallic Fe in the sample of USP100-1200, which was expected because Fe-saturation was imposed during synthesis of this sample. However, for USP75 and USP80, it is not clear what the origin of this impurity is. It may be indicative of microscale inhomogeneity and/or the presence of a trace of metallic Fe in these specimens. The magnetization curves of USP75, before and after annealing, were also anomalous, with curvilinear magnetization trends continuing up to the highest field applied. This probably is indicative of proximity to the Curie temperature in these specimens. The constricted loops may indicate particle-size variation and/or compositional inhomogeneity (Wasilewski et al., 1975). Annealed specimens had much lower coercive force, and constrictions were virtually absent from the loops determined for these samples. Saturation moments are reported in Table 6.

Table 5. Thermal ellipsoids of oxygen atoms

	USP75-1350	USP75-1350,800A	USP100-1200
RMS displacement (Å) parallel to [111]	0.092(4)	0.098(4)	0.093(4)
RMS displacement (Å) perpendicular to [111]	0.116(3)	0.124(1)	0.146(2)

Table 6. Unit-cell parameters and magnetic moments

Sample ID	a(Å)	μ^A_{Fe}/μ^B_{Fe}	M_{net} (μ_B)	M_s (emu/g)	M_s (μ_B)
MT100-1350	8.3958(2)	1.084(16)	3.39	92.2	3.82
MT100-1350,800A	8.3953(2)				
USP25-1350	8.4237(2)	1.085(29)	2.33	63.2	2.60
USP25-1350,800A	8.4236(3)	1.048(14)	2.49	63.9	2.63
USP50-1350	8.4625(2)	1.040(46)	1.38	38.9	1.58
USP50-1350 (77 K)	8.440(5)*	1.051(25)	1.68		
USP50-1350,800A	8.4628(2)	1.023(29)	1.43	39.0	1.59
USP75-1350	8.5073(1)				
USP75-1350,800A	8.5068(2)				
USP100-1200	8.5348(2)				
MT100-930	8.3954(2)			91.8	3.81
USP10-930	8.4042(1)				
USP20-930	8.4172(1)			68.3	2.81
USP30-930	8.4312(2)				
USP40-930	8.4465(2)			49.4	2.02
USP60-930	8.4785(1)			28.8	1.17
USP70-930	8.4960(2)				
USP72.5-930	8.5005(2)				
USP75-930	8.5048(3)				
USP77.5-930	8.5080(1)				
USP80-930	8.5110(2)				

Determined from profile refinement of neutron diffraction pattern.
All measurements at room temperature except where indicated.
μ^A_{Fe}/μ^B_{Fe} *and* M_{net} *derived from neutron diffraction results.*
M_s *values from magnetometer measurements.*

Electron microprobe analyses

Samples of MT100, USP25, USP50, and USP75 synthesized at 1350°C were analyzed by electron microprobe. Annealed specimens of USP25 and USP75 were also examined. The microprobe was operated at 15 kV, 0.015 μA sample current on brass, using a 400,000 count beam integration, a beam spot size of about 1 μm, and a synthetic Usp_{50} working standard. Data reduction followed the procedures of Bence and Albee (1968) and Albee and Ray (1970). Individual spot analyses were performed on from 15–23 grains in each specimen. The samples were found to be homogeneous on the scale of the beam diameter. Averages of the individual analyses are reported in Table 7. Clearly, each specimen has the correct Fe/Ti ratio for the nominal composition. No difference was found for the specimens after annealing. Qualitative energy-dispersive analysis did not reveal the presence of chemical impurities in any of the specimens.

Results

Unit-cell parameters

Unit-cell parameters were determined for all specimens using two-theta values collected on an automated powder

Table 7. Electron microprobe analyses

	FeO(wt.%)	TiO_2(wt.%)	Mole % Fe_2TiO_4	No. of Analyses
MT100-1350	92.4(4)	---	0.0	23
USP25-1350	84.6(3)	8.5(1)	24.9(3)	17
USP25-1350,800A	84.8(4)	8.5(1)	24.8(3)	16
USP50-1350	78.9(4)	17.8(2)	50.6(4)	23
USP75-1350	70.7(4)	26.3(3)	75.1(6)	15
USP75-1350,800A	70.7(3)	26.2(2)	75.0(6)	15

Values quoted are the mean and standard deviation for the number of individual spot analyses shown.
All Fe reckoned as FeO.
Mole % Fe_2TiO_4 calculated assuming R_3O_4 stoichiometry.

X-ray diffractometer, using the procedures described by Wechsler (1981). The positions of 13 Cu$K\alpha_1$ reflections between 30 and 90° two-theta were included in the least-squares refinement program CPLSQ (Wechsler, 1981). In addition to the cell edge, a systematic error correction for sample displacement was refined for each set of data.

Unit-cell parameters are reported in Table 6 and Figure 1. The trend is essentially an s-shaped curve similar to that reported by Lindsley (1965) for samples prepared hydrothermally at 800°C and Banerjee et al. (1967) for specimens sintered at 1100°C in evacuated silica tubes. The present results strongly suggest that the trend is continuous between x = 0 and x = 0.75, with curvature gradually decreasing toward x = 0.75. These data are also suggestive of a relatively sharp break at about x = 0.75 followed by a possibly linear trend to x = 1.0. This discontinuity may be indicative of nonstoichiometry (cation deficiency) in the specimens with x > 0.75. It should be noted, however, that at room temperature the titanomagnetites undergo a transition from paramagnetic to ferrimagnetic in the vicinity of x = 0.75, which might also contribute to the change in slope in this region.

No significant change in cell parameter was detected for specimens annealed at 800°C following quenching from 1350°C, nor is there any difference between the trends observed for samples (x = 0, 0.25, 0.5) synthesized at high temperature under controlled fo_2 conditions and those synthesized at 930°C in evacuated silica tubes. The cell parameters for USP75 prepared at 1350°C (before and after annealing), however, are significantly larger than that of USP75 made at 930°C. The reason for this is not certain. A possible explanation is that the wüstite-saturated spinel at 1350°C has a cation excess relative to the 930°C specimen. This would be in accord with the change in composition of the spinel in equilibrium with Fe^0 + wüstite between 1000 and 1300°C reported by Simons and Woermann (1978). An alternative possibility is that the 1350°C USP75 is ~2 mole % more Fe_2TiO_4-rich than the 930°C sample, although no such variation was detected in the microprobe analyses (Table 7).

Although Akimoto et al. (1957) suggested a nearly linear dependence of the cell parameter on composition and Bleil (1976) proposed a straight line as the best fit to the *a*–x data, the present measurements confirm with a high degree of certainty that the deviation from linearity is significant. Akimoto et al.'s cell parameter measurements, though showing a somewhat greater scatter than those reported here, are, in fact, consistent with this trend.

O'Reilly and Banerjee (1965) claimed that changes in slope near x = 0.2 and x = 0.8 supported their model for the cation distribution in titanomagnetites. More recently, Newton and Wood (1980) have advanced a similar argument based upon assumed cation preferences for the tetrahedral and octahedral sites to explain the observed trend. However, results presented below do not support the contention that the cell parameter variation is controlled by changes in the cation distribution with composition, and an alternative explanation will be proposed.

Space group

The spinel structure has space group *Fd3m*. This space group requires equivalence among octahedral sites and among tetrahedral sites, at least as averaged over the diffracting volume. For spinels in which different types of cations occur together on the same sites, this implies a random distribution of the cations over equivalent sites. When such equivalence is violated, the cations may order in a variety of ways, reducing the symmetry. Haas (1965) has derived the possible space group transformations which may result from various ordering schemes among the spinel A and B sites.

Previous neutron and X-ray diffraction studies of magnetite (e.g., Hamilton, 1958; Fleet, 1982), ulvåospinel (Ishikawa et al., 1971; Forster and Hall, 1965), and

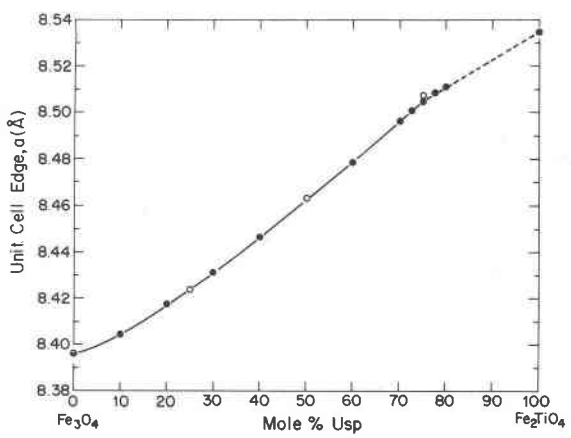

Fig. 1. Variation of unit-cell parameters with composition for titanomagnetites synthesized in this study. A portion of the line is dashed because the "100% Fe_2TiO_4" specimen is actually nonstoichiometric. Open symbols indicate samples synthesized at 1350°C in a controlled atmosphere, solid symbols indicate samples synthesized in evacuated silica tubes at 930°C (1200°C for "Usp_{100}").

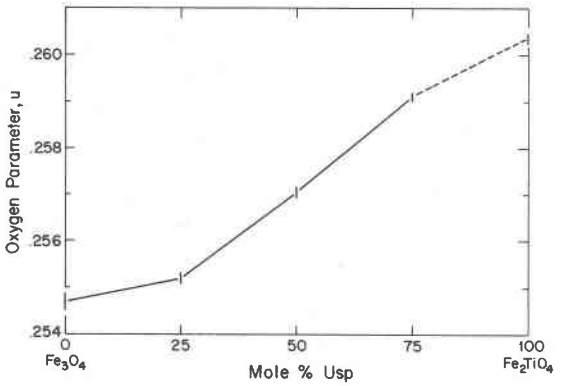

Fig. 2. Oxygen parameter values from neutron diffraction structure refinements.

intermediate titanomagnetites (Ishikawa et al., 1964), have found no evidence contradicting the assumption of *Fd3m* symmetry. However, powder patterns obtained in the present study are considerably better resolved than those of earlier studies. Although powder patterns are generally not the ideal means of determining space group symmetry, neutron diffraction does provide a sensitive test for ordering of Fe and Ti, as well as Fe^{2+} and Fe^{3+}, in titanomagnetites. Any such ordering would result in readily visible superstructure lines in the powder pattern.

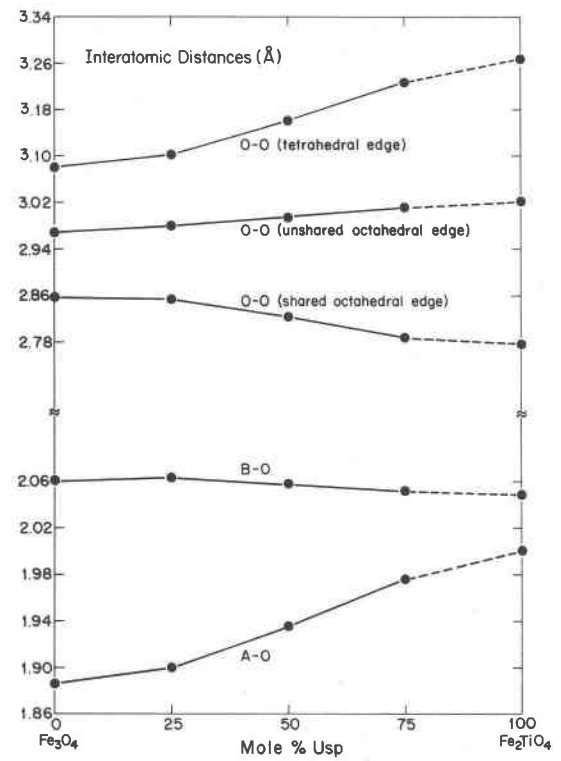

Fig. 3. Variation of selected interatomic distances with composition.

No such extra reflections or splitting of spinel peaks was observed. All the patterns were consistent with *Fd3m*, including the 77 K data on USP5O. However, as will be discussed more fully below, observations of diffuse scattering and large temperature factors may indicate local symmetry lower than *Fd3m*.

Positional parameters

Only one positional parameter is variable in *Fd3m*, the oxygen coordinate, u. Refined values of u are listed in Table 3 and shown in Figure 2, and the resulting interatomic distances and angles are given in Table 4 and Figure 3. For comparison, other values of u reported for titanomagnetites are listed in Table 8. In general, the agreement with other reported values is good. The value $u = 0.256$ for $x = 0.56$ reported by Ishikawa et al. (1964) appears rather low; however, their value is uncertain due to the lack of an extinction correction on their single-crystal data. The value of u for a natural titanomagnetite with 59 mole % Fe_2TiO_4 (Stout and Bayliss, 1980) is considerably different from the trend reported here, although values for two other natural titanomagnetites are much more similar. The data of Fujino (1974) are in good agreement with the present results except for the most Fe_2TiO_4-rich compositions. These may well be complicated by varying degrees of nonstoichiometry in different suites of samples prepared by different methods.

The trend of the data shown in Figure 2 is suggestive of an s-shaped curve describing the dependence of u on composition, similar to that obtained for the cell parameter. Interpretation of the Usp-rich portion of these curves is, however, complicated by the known nonstoichiometry of the USP100–1200 specimen. In Figure 4, the data are shown in terms of a vs. u and A–O vs. B–O distance. Clearly, the trend is linear from $x = 0.25$ to $x = 1.0$, but changes slope significantly between $x = 0$ and $x = 0.25$. Since these two parameters alone give a complete description of the average crystal structure, it is thus evident that a major change in the way the structure responds to varying composition occurs in the low-Ti region of the series. Possible reasons for this change in behavior will be discussed below.

The oxygen parameter was identical for annealed and unannealed specimens with $x = 0.25$, $x = 0.5$, and $x = 0.75$, suggesting that no change in cation distribution occurred as a result of annealing.

Temperature factors

For all refinements, an individual isotropic or anisotropic temperature factor was refined for each site (Tables 3 and 5, Fig. 5). Clearly, the values of B for each site increase significantly with increasing Fe_2TiO_4 content. The octahedral site B increases least rapidly, while the oxygen temperature factor increases the most. This probably reflects static positional disorder of the atoms as a result of mixing of Fe and Ti on octahedral sites. Similar

Table 8. Oxygen parameter values for titanomagnetites

Mole % Fe_2TiO_4	u*	Comments	Reference
0	0.254(1)	Natural, single crystal, x-ray diffraction	Claasen (1926)
0	0.2548(2)	Synthetic, single crystal, neutron diffraction	Hamilton (1958)
0	0.2542(9)	Synthetic, powder, x-ray diffraction	Fujino (1974)
0	0.2552(4)	Natural, single crystal, x-ray diffraction	Yakel (1980)
0	0.2549(1)	Natural, single crystal, x-ray diffraction	Fleet (1981)
23	0.2553(6)	Synthetic, single crystal, x-ray diffraction	Fujino (1974)
24	0.2556(10)	Synthetic, powder, x-ray diffraction	Fujino (1974)
48	0.2568(10)	Synthetic, powder, x-ray diffraction	Fujino (1974)
56	0.256	Synthetic, single crystal, neutron diffraction	Ishikawa *et al.* (1964)
58	0.2587(7)	Synthetic, single crystal, x-ray diffraction	Fujino (1974)
59	0.2620(2)	Natural, single crystal, x-ray diffraction	Stout and Bayliss (1980)
62	0.2587(10)	Synthetic, powder, x-ray diffraction	Fujino (1974)
70	0.2594(4)	Synthetic, single crystal, x-ray diffraction	Fujino (1974)
73	0.2609(10)	Synthetic, powder, x-ray diffraction	Fujino (1974)
73	0.2599(2)	Natural, single crystal, x-ray diffraction	Stout and Bayliss (1980)
74	0.2595(2)	Natural, single crystal, x-ray diffraction	Stout and Bayliss (1980)
87	0.2613(10)	Synthetic, powder, x-ray diffraction	Fujino (1974)
90	0.2611(9)	Synthetic, powder, x-ray diffraction	Fujino (1974)
92	0.2614(2)	Synthetic, single crystal, x-ray diffraction	Fujino (1974)
95	0.261(1)	Synthetic, single crystal, neutron diffraction	Ishikawa *et al.* (1971)
99	0.261(1)	Synthetic, powder, neutron diffraction	Ishikawa *et al.* (1964)
100	0.265(10)	Synthetic, powder, x-ray diffraction	Barth and Posnjak (1932)
100	0.261(1)	Synthetic, powder, neutron diffraction	Forster and Hall (1965)

*All values referred to choice of unit-cell origin at center of symmetry.

observations were also made by Fujino (1974). This interpretation is also suggested by comparing the temperature factors determined for USP50–1350 at 298 K and 77 K (Fig. 6). The octahedral site B extrapolates to near zero at 0 K as expected if the displacements are due only to thermal motion, whereas B's for the tetrahedral site and oxygen have values of about 0.4 and 0.5, respectively, at 0 K. These values indicate that a significant portion of the atomic displacements may be due to distortions from the average structure rather than thermal motion.

The orientations of thermal ellipsoids refined for USP75 and USP100 (Table 5) indicate that displacement of the oxygen from its mean position is much greater within the (111) plane than perpendicular to it. In fact, the

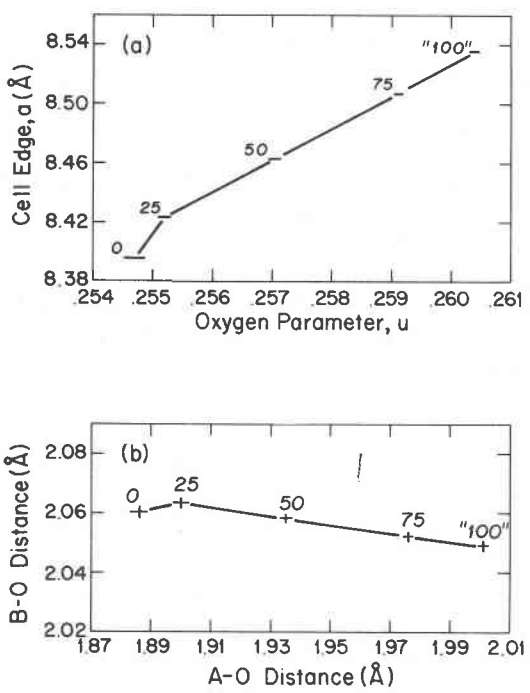

Fig. 4. (a) Unit-cell edge vs. oxygen parameter. (b) A–O distance vs. B–O distance. Numbers indicate mole % Fe_2TiO_4.

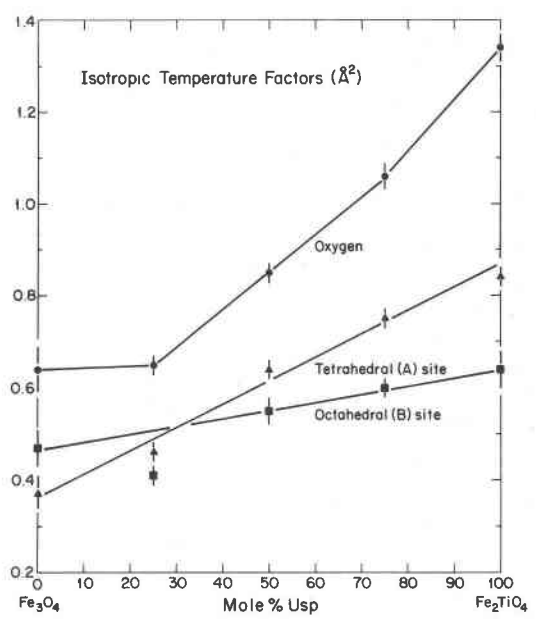

Fig. 5. Variation of isotropic or equivalent isotropic temperature factors of tetrahedral, octahedral, and oxygen sites with composition. Values shown for intermediate compositions are those determined on annealed specimens.

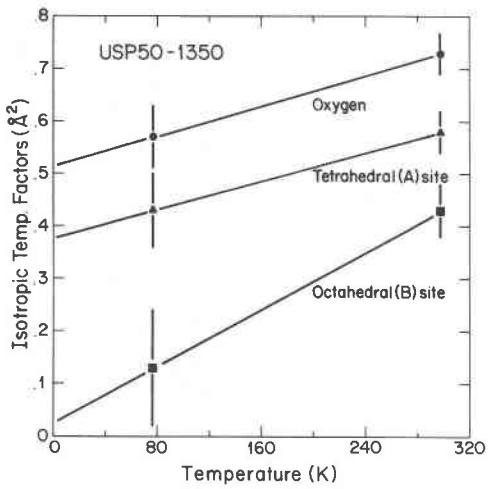

Fig. 6. Isotropic temperature factors of USP50–1350 at room temperature and 77 K.

RMS displacement of oxygen perpendicular to (111) is essentially identical in USP75 and USP100 to that in pure magnetite, suggesting that all of the excess (nonthermal) contribution to the displacement in these materials occurs within the (111) plane.

Temperature factors determined for the annealed specimens of USP50 and USP75 were slightly higher than those before annealing. However, the values for USP25 were equal (for A-site and oxygen) or slightly less (for the B site) after annealing than before.

Magnetic moments

Shull et al (1951) confirmed the Néel-type ferrimagnetic ordering scheme in magnetite. Later studies of magnetite (e.g., Hamilton, 1958) and titanomagnetites (Ishikawa et al., 1964, 1971) were also consistent with this magnetic ordering, as are saturation magnetization measurements. Although powder neutron diffraction techniques do not provide any information on the orientation of the magnetic moments in the structure (Shirane, 1959), they do yield information on the magnitude of the moments as well as confirming the type of ordering.

The net spontaneous magnetization, assuming colinear ferrimagnetic ordering with A and B sites coupled antiparallel to one another, is given in Table 6 for MT100, USP25, and USP50. These values are somewhat lower (by ~5–10%) than the saturation magnetization determined at room temperature (Table 6, Fig. 7). Overall, the net magnetic moments and saturation magnetization values display an essentially linear trend with composition, with no difference between the 1350 and 930°C suites of specimens.

The individual site moments are significantly lower than might be expected at room temperature. The value $\mu_{Fe}^{A} = 4.01\ \mu_B$ in MT100–1350 is only 80% of the theoretical spin-only 0 K moment of 5 μ_B expected for Fe^{3+} in purely inverse magnetite. Studies of the temperature dependence of the sublattice magnetizations in magnetite (Riste and Tenzer, 1961; van der Woude et al., 1968) have been limited to room temperature and above, but Mössbauer spectra collected at room temperature and low temperature for magnetite (Banerjee, O'Reilly, and Johnson, 1967; Kundig and Hargrove, 1969; Hargrove and Kundig, 1970; Dickof et al., 1980) suggest 94–96% saturation of the A site Fe^{3+} moment at room temperature. The site magnetizations determined here for USP50 at 77 K are only about 90% of those that would be expected for the moments at 0 K.

Some of this discrepancy may lie in the effects of covalent contributions to the bonding, resulting in magnetic moments lower than those expected for the free ions. Sawatzky and van der Woude (1974) calculated moments of 4.31 and 4.62 μ_B for A and B site Fe^{3+} in ferrites, including covalency, and Dickof et al. (1980) observed a magnetic moment of $4.55 \pm 0.06\ \mu_B$ for B site Fe^{3+} in magnetite from magnetization data on zinc-substituted magnetites. The observed moments for the A and B site Fe in magnetite in this study are not inconsistent with such values. However, the fact that the net moments derived from neutron diffraction are about 0.1–0.4 μ_B (5–10%) lower than the magnetometer results obtained here indicates there may be other factors contributing to the discrepancy. The refined magnetic moments could perhaps be slightly underestimated due to uncertainties in the magnetic form factor and the lack of corrections for absorption and thermal diffuse scattering. It is also possible, however, that the spontaneous magnetization at zero applied field, as determined by neutron

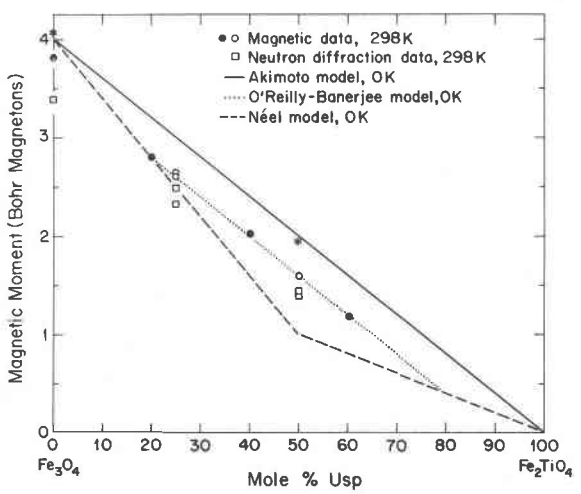

Fig. 7. Values of saturation magnetization (circles) and net magnetic moments derived from neutron diffraction results (squares) at room temperature. Asterisks represent estimated magnetic moments at 0 K of two samples. Open symbols indicate samples synthesized at 1350°C, solid symbols indicate samples synthesized at 930°C.

diffraction, is appreciably lower than the saturation magnetization measured at essentially infinite applied field due to the presence of domain boundaries, local compositional inhomogeneities, or other defects.

In order to estimate the Fe^{2+}–Fe^{3+} occupancies from site magnetization data obtained at room temperature, it is necessary to know the actual ionic moments at 0 K and the temperature dependence of the magnetic moment of each species on each site for all compositions. In the absence of sufficient experimental data, the following approximations can be made: (1) the Fe^{2+} and Fe^{3+} magnetic moments are independent of which site the ions occupy; and (2) $\mu_{Fe^{2+}} = (4/5)\mu_{Fe^{3+}}$ at all temperatures. The ratio μ^A_{Fe}/μ^B_{Fe} (where μ_{Fe} is the average magnetic moment for all Fe species on a given site) then uniquely determines the cation distribution. The observed values (Table 6) are very nearly those which would be expected for the Akimoto distribution (Fig. 8). The value for USP50 at 77 K is essentially identical to that at room temperature, suggesting that the approximation of equal temperature dependencies of the magnetic moments on the two sites is valid, at least for this composition. Although the assumptions used in this calculation are probably not rigorously correct, the observed trend is certainly consistent with and suggestive of a cation distribution similar to that predicted by the Akimoto model.

The results also indicate no significant difference in the individual site moments for USP25 and USP50 before and after annealing. However, in both cases, the small changes in the parameters result in decreased μ^A_{Fe}/μ^B_{Fe} after annealing, and a slight increase in net moment. Magnetometer measurements reveal a significant decrease in coercivity and a faster approach to saturation in the annealed specimens, but virtually identical saturation moments. Such changes are not consistent with any increase in cation ordering as a result of the annealing. The observed changes probably reflect annealing out of defects and improved homogeneity rather than any change in cation ordering.

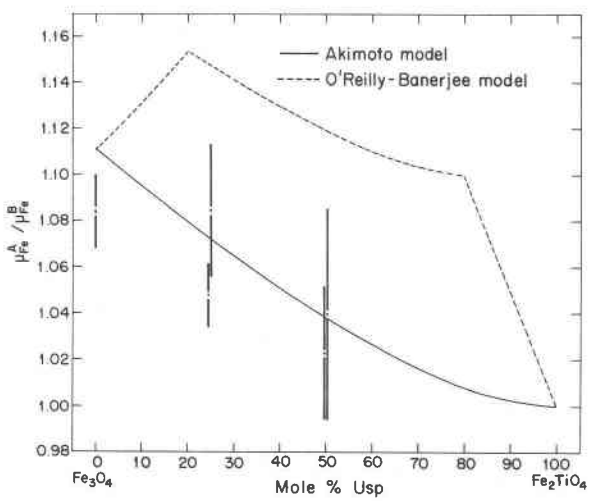

Fig. 8. Ratio of magnetic moments for Fe on A and B sites for 5 specimens studied by neutron diffraction and two theoretical models.

Occupancy refinements

Since the suggestions by Gorter (1957) and Akimoto et al. (1957) regarding the possibility of Ti in the tetrahedral site of titanomagnetites, many investigators have addressed this question. Forster and Hall (1965) concluded from X-ray and neutron diffraction data that ~9% of the Ti in their specimen of (nominally) Fe_2TiO_4 was in the tetrahedral site. However, Ishikawa et al. (1964, 1971) and Fujino (1974) detected no tetrahedral Ti. More recently, Stout and Bayliss (1980) suggested the presence of tetrahedral Ti in a natural titanomagnetite based on X-ray structure refinements, although in two other natural specimens they found no evidence for tetrahedral Ti. Magnetic data on titanomagnetites can all be reasonably well explained assuming all Ti is octahedral, although such measurements do not prove this contention.

Occupancy refinements were performed on all neutron diffraction data with two objectives in mind: to determine whether any Ti was present in the tetrahedral site, and to check the total occupancy of Ti against the nominal compositions of the samples. The first of these was accomplished by varying the occupancy of tetrahedral Ti, while constraining the total Ti content and the total occupancy of both sites. The second was studied by varying the octahedral site Ti occupancy only, keeping the total octahedral site occupancy of Fe + Ti fixed, and tetrahedral Ti fixed at zero.

In USP25, USP50 and USP75, both annealed and unannealed specimens gave refined values of Ti (tetrahedral) within two esd's of being zero. Because of the large difference in neutron scattering cross sections between Fe and Ti, this result is extremely significant, with esd's of 0.003–0.007 cations per tetrahedral site. For USP100, the occupancy cannot be determined as easily because of the assumed presence of cation vacancies whose fractional occupancies on the two sites are also unknown. The refinements for this sample are consistent with the vacancies being distributed approximately equally over both tetrahedral and octahedral sites, with all Ti octahedral, or with the vacancies being all octahedral and a small amount of Ti ($\leq$1%) in the tetrahedral site. Models in which the tetrahedral Ti is greater than this or in which the vacancy is entirely tetrahedral can be rejected. This result is particularly interesting since the Ti content of this specimen is 1.035 cations per 4 oxygens, greater than that of stoichiometric ulvöspinel.

All refinements of total Ti, with $Ti_A = 0$ and $(Fe+Ti)_B = 2$, gave occupancies of Ti no more than 2 esd's from the nominal composition, with most esd's $\leq$0.01. Therefore, final refinements kept Ti entirely in the octahedral site and fixed at the nominal occupancy expected for the

given composition. No significant change was found for samples before and after annealing, although changes in composition of 1–2 mole % Fe_2TiO_4 would not be inconsistent with these findings.

Previous reports of tetrahedral Ti in titanomagnetites are probably spurious. In the case of Forster and Hall's (1965) result, their specimen was most likely nonstoichiometric, and the deviation from their assumed composition may have resulted in the apparent tetrahedral Ti. The results of Stout and Bayliss (1980) may indicate the presence of a small amount of a lighter element in the tetrahedral site. However, a plausible alternative to tetrahedral Ti is that some Mg, Al, and/or Si, which they assigned to the octahedral site, are actually present in the tetrahedral site. Their reported microprobe analyses indicate the presence of sufficient quantities of these elements to account for this effect.

Diffuse scattering

Background levels were determined for all powder patterns by averaging from 10–20 point intensities (0.5–1° two-theta) at clear portions of the patterns. Since the spinel pattern is relatively uncomplicated, the background is quite well determined, even at high angles, where some peak overlap occurs. The background estimate for USP100–1200 is shown in Figure 9. Several areas of diffuse scattering are present. These were found in all the Ti-bearing specimens, and were seen to increase in intensity with increasing Ti concentration as well as with annealing.

Although the origin of this diffuse scattering is not fully understood, it almost certainly arises from local deviations from the average structure. The greatest contribution to this scattering probably is due to the mixing of Fe and Ti on the octahedral site. The increase in diffuse intensity observed following annealing may be indicative of slight changes in cation ordering and suggests the possibility that short-range order among octahedral cations may be present. Short-range order might develop with increasing Ti content as a result of the greater electrostatic repulsive potential between neighboring octahedral sites. With local order in a tetragonal ($P4_122$) or orthorhombic (*Imma*) configuration, the number of near-neighbor Ti ions surrounding a given Ti ion can be reduced relative to a random distribution among the octahedral sites, thus minimizing the electrostatic repulsive potential. Calculated powder patterns indicate that the tetragonal variant is more likely to produce the observed distribution of diffuse scattering, although other local ordering arrangements, perhaps of lower symmetry, might also be present and contribute to the diffuse scattering.

The presence of short-range order in inverse spinels has been predicted on the basis of energy considerations (e.g., deBoer et al., 1950; Anderson, 1956). Powell and Powell (1977) suggested short-range order effects to explain the approximate ideality of titanomagnetite solid solutions at high temperature with a molecular mixing model. Jacob and Alcock (1975) and Wechsler and Navrotsky (1982) found evidence of short-range order in Zn_2TiO_4 and Mg_2TiO_4, respectively, from thermochemical data. Furthermore, Mg_2TiO_4, Mn_2TiO_4, and Zn_2TiO_4 spinels have been observed to transform to the $P4_122$ ordered structure at low temperatures (Vincent et al., 1966; Delamoye and Michel, 1969; Wechsler and Von Dreele, 1983). Thus, although the present observations of diffuse scattering are not conclusive, there is at least permissive evidence that short-range order may be of considerable importance in titanate spinels. As will be discussed more fully below, the crystallographic and magnetic properties of titanomagnetites are also consistent with this interpretation.

Discussion

The trends reported here for the variation of the unit-cell parameter, oxygen parameter, and magnetic moments as a function of composition do not support the contention of a quenchable temperature-dependent cation distribution in titanomagnetites as proposed by Stephenson (1969) and Bleil (1971, 1976). No significant difference was found for any of these measured properties as a result of synthesis (quenching) temperature, or post-synthesis annealing. The magnetization data suggest strongly that the average Fe^{2+}–Fe^{3+} distribution is highly disordered in these specimens, and is probably quite similar to the Akimoto model. Of course, the possibility that a high-temperature distribution was retained metastably during annealing at 800°C and was created metastably during synthesis at 930°C cannot be absolutely ruled out, but seems unlikely.

Although room-temperature saturation magnetization

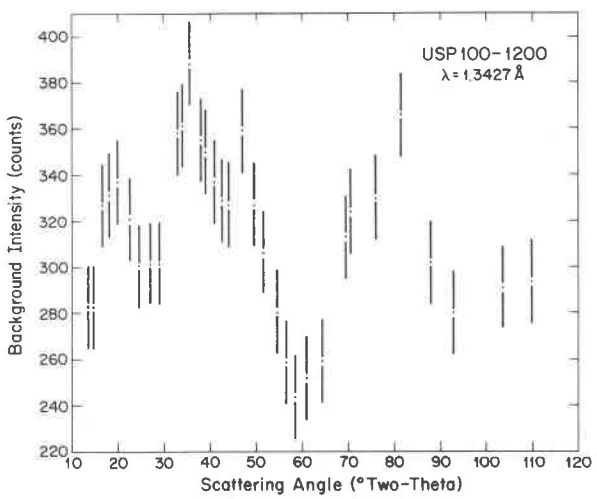

Fig. 9. Estimate of background intensity of neutron diffraction pattern for USP100–1200. Error bars are equal to ± square root of the average background count.

data lie somewhat below the trend predicted for the Akimoto distribution model (Fig. 7), it is important to recognize that magnetization is reduced by thermal disorder at temperatures above 0 K. Estimates can be made of the 0 K moments of two of these specimens. The room temperature moment observed for magnetite is comparable to values reported elsewhere (see Smit and Wijn, 1959), and it can thus be expected that the 0 K saturation moment will be in the vicinity of 4.1 μ_B. For USP50, neutron diffraction experiments suggest an increase in the net moment of 0.3 μ_B, or about 20%, between room temperature and 77 K. Therefore, the extrapolated saturation moment at 0 K is likely to be on the order of 1.9–2.0 μ_B, suggesting that the cation distribution is very nearly that expected for the Akimoto model, which predicts a value of 2.0 μ_B for this composition.

The present results are also consistent with suggestions that the Fe^{2+} and Fe^{3+} magnetic moments (extrapolated to 0 K) are somewhat lower than the theoretical spin-only values of 4 and 5 μ_B, perhaps resulting from covalency effects. Thus, actual site occupancies cannot be precisely inferred from magnetization measurements assuming the theoretical moments, since such measurements give only the net moment, i.e., the difference between octahedral and tetrahedral site magnetizations. Nevertheless, the essentially linear trend in magnetization found in this study and in several previous low-temperature magnetic studies gives a strong indication that the Fe^{2+}–Fe^{3+} site occupancies vary approximately linearly with composition. The A and B-site moments determined by neutron diffraction also support this conclusion. On the other hand, a slight octahedral preference for Fe^{2+} (= tetrahedral preference for Fe^{3+}) in the low-Ti region would also be consistent with both the magnetic and crystallographic properties determined in this study and cannot be ruled out.

Earlier studies have suggested that apparent discontinuities in the dependence of cell parameter upon composition, as well as breaks in other trends, were an indication of changes in the cation distribution. However, the data presented here suggest a continuous cation substitution scheme in which the tetrahedral and octahedral site occupancies vary essentially linearly with composition. The nonlinear variations of the cell parameter and oxygen parameter with composition can perhaps be reconciled to this cation distribution by considering the possible importance of octahedral cation interactions.

In the spinel structure, the parameters a and u are sufficient to describe fully the structural topology. The oxygen parameter is commonly thought of as an expression of the ratio of tetrahedral to octahedral cation-oxygen distances, while the cell parameter expresses the overall volume of the structure. Studies of spinel systematics (Hill et al., 1979) indicate that as much as 97% of the variability in a and u can be explained on the basis of assumed cation radii (Shannon, 1976). Nevertheless, other structural elements are directly related to the parameters a and u and may have significant effects on their values. Specifically, the A–A, B–B, and A–B distances are directly proportional to a, while the lengths of the tetrahedral and octahedral edges are related to both a and u. The octahedral site has two nonequivalent edges, one shared with neighboring octahedral sites and the other unshared. The relative lengths of these edges are related to u, with increasing u indicating a shortening of the shared edge relative to the unshared edge.

While the A–A and A–B distances are fairly long, 3.5–3.7Å, the B–B distance, which varies from approx. 2.97Å in magnetite to 3.02Å in ulvöspinel, is short enough to result in possibly significant interactions between octahedral cations. Indeed, the electron delocalization or hopping found in magnetite is testimony to the existence of such interactions. Any interaction with a tendency to increase the average B–B separation must result in a lengthening of the cell edge. Similarly, increased B–B repulsion would also be likely to result in a relative shortening of the shared octahedral edge and thereby to increase u as well.

The s-shaped trends in a and u vs. composition (Figs. 1 and 2) indicate greater dependence of these properties on composition with increasing Ti content (up to $x \simeq 0.75$). Furthermore, the variation of a with u (Fig. 4a) suggests that a significant change in behavior takes place in the low-Ti region of the titanomagnetite series. Two possible mechanisms that might take effect at low Ti concentrations are proposed to explain these observations.

First, the presence of Ti^{4+} ions in adjacent octahedral sites may cause a significant increase in the B–B repulsive potential. For a statistically random distribution of Fe and Ti among the octahedral sites, Ti–Ti pairs would always exist in neighboring octahedral sites at compositions with $x > 1/3$, although even for $x < 1/3$, the probability of finding Ti in adjacent sites would still be finite. The increased repulsion that might result from such interactions could contribute to the observed increasing dependence of a and u on composition.

Second, the presence of small amounts of Ti may inhibit the electron delocalization of octahedral Fe. If this were to result in relatively greater repulsion (or less attraction) between the octahedral cations, this effect might also help to explain the observed crystallographic changes.

The effect of Ti–Ti repulsions might be mitigated by the development of short-range order, thereby accounting for the change in slope of the a and u vs. x curves at higher Ti concentrations. A second factor that may contribute to the relatively sharp break in these trends near $x = 0.75$ is nonstoichiometry. It is possible that the relatively high coordination of Ti by other Ti ions in close proximity requires a relatively large volume increase. This might be responsible for the instability of stoichiometric spinel relative to Fe^0 + cation-deficient spinel as observed in

phase equilibria experiments near the Fe_2TiO_4 end-member by Simons and Woermann (1975).

The Akimoto model requires that exactly 1/2 of the octahedral sites be occupied by Fe^{2+} for all compositions and that Fe^{3+} (A) exactly equals Fe^{3+} (B). For this distribution to be attained without any symmetry constraints (i.e., splitting of equivalent sites into nonequivalent sites, thereby lowering the space group symmetry) inconsistent with *Fd3m* is remarkable and requires crystal-chemical justification. One possible explanation for the establishment of this distribution requires the assumption that the structure is energetically most stable when the octahedral site contains no more than one (Fe^{3+} + Ti^{4+}) per formula unit. Assuming Ti^{4+} has a strong octahedral site preference, this implies that the maximum acceptable amount of octahedral Fe^{3+} is always present. This may be controlled, or at least influenced, by a tendency toward maintaining equal numbers of Fe^{2+} and Fe^{3+} ions on the octahedral sites, subject to the above constraints. Such an arrangement may be favored by a tendency toward electron delocalization between Fe^{2+} and Fe^{3+}, which is clearly evident in magnetite at room temperature and may be present in titanomagnetites as well. Similar observations have been made by Robbins et al. (1971) for the system $Fe_{3-x}Cr_xO_4$ and by Evans et al. (1976) in $Fe_{3-x}Sn_xO_4$.

Another solution to the problem of establishing the Akimoto distribution is the possibility of short-range order. In general, the symmetry at a given octahedral site must be lower than $\bar{3}$m (octahedral site symmetry of the average structure) because of the near neighbor cation distribution. It is conceivable, then, that the octahedral sites might become energetically nonequivalent, so that half the sites are favorable for Fe^{2+}, and the remaining sites are favorable for Fe^{3+} and Ti^{4+}. This could produce an Akimoto-type distribution without requiring long-range order. The requirements of local charge balance may favor cation ordering. Such short-range order might also be enhanced by a tendency toward pairwise interactions between Fe^{2+} and Fe^{3+}, since a locally ordered arrangement would allow greater near-neighbor coordination of octahedral cations by other octahedral cations of a differing species, relative to a random distribution.

A further question that remains unanswered is whether the Akimoto distribution truly represents the high-temperature limit for cation disorder or whether a more random distribution may be stable at high temperatures. The transition to a statistically random Fe^{2+}–Fe^{3+} distribution requires only the transfer of an electron between Fe on the A and B sites. Numerous studies suggest the importance of thermally-activated electron delocalization in Fe-bearing minerals (see Burns et al., 1980). In addition, Mössbauer spectra suggest the loss of discrete Fe^{2+}–Fe^{3+} species at ~600°C in magnetite (Evans, 1973). Whether the electron delocalization also involves Fe in the A-site is uncertain, but thermoelectric measurements (Wu and Mason, 1981) support a truly random distribution in Fe_3O_4 at high temperature.

It is interesting to speculate in this connection that the apparent discontinuity in thermochemical properties of coexisting titanomagnetites and hematite–ilmenites in the vicinity of 850°C might be related to the transition between a statistically random distribution of Fe^{2+}–Fe^{3+} (and/or Fe–Ti) at high temperature to Akimoto-type ordering at low temperature. If the cation distribution has, in fact, been quenched from high temperature, then the results presented here suggest that statistical disorder may not be approached even at 1350°C. It seems more plausible, however, to view the electrons as being sufficiently mobile that equilibrium may be established at relatively low temperature, and that the high-temperature distribution cannot be quenched in.

If the Akimoto distribution is indeed the actual configuration for the titanomagnetite series, then previous low-temperature magnetization measurements on synthetic specimens that gave saturation moments significantly lower than the Akimoto model (Akimoto et al., 1957; O'Reilly and Banerjee, 1965; Bleil, 1976) may have been in error. Most of these specimens were synthesized from oxide mixes in evacuated SiO_2-glass tubes at 1100–1150°C for 6–20 hours. One suite of samples (Bleil, 1976) was synthesized in a controlled atmosphere at 1100°C, but no further details of synthesis procedures were given. Jensen and Shive (1973) have suggested that the disparity in saturation moments may be due to incomplete homogenization of the synthetic materials. More recently, Lawson (1978) also noted difficulties in producing homogeneous single phases in the hematite-ilmenite system using the evacuated SiO_2 tube sintering process.

The correspondence in saturation magnetization values and unit-cell parameters for specimens prepared by different techniques at temperatures between 800 and 1350°C suggests that a reasonably close approach to equilibrium was probably achieved in the materials studied here. Discrepancies between these results and some previous studies can probably be ascribed largely to the difficulties involved in preparing homogeneous unoxidized titanomagnetites.

Another possibility must also be taken into consideration, however. The materials synthesized at 1350°C in this work were prepared in gas mixtures selected to impose wüstite saturation in the spinel phase. The study of Aragón and McCallister (1982) suggests that titanomagnetites in equilibrium with wustite have a slight cation excess. It is likely that both the thermodynamics and kinetics of cation ordering in titanomagnetites are sensitive to variations in cation/anion ratios, and therefore some of the differences between cation distributions infrerred in this and other studies could be due to differences in the degree of cation or anion excess.

Conclusions

Crystallographic and magnetic properties were determined for a suite of synthetic titanomagnetites. No significant differences were found in the unit-cell parameters, oxygen positional parameters, or magnetization as a result of different synthesis temperatures (930 and 1350°C) or annealing (800°C for up to 95 days). These results do not support models that propose a quenchable temperature-dependent Fe^{2+}–Fe^{3+} distribution. Rather, the saturation magnetization and individual sublattice magnetic moments suggest that all of the specimens have a cation distribution similar to that proposed by Akimoto (1954). All Ti was confirmed to be in the octahedral position. The significantly larger temperature factors observed for Fe_2TiO_4-rich compositions suggest the presence of a considerable degree of positional disorder, presumably due to the mixing of Fe and Ti on the octahedral sites.

Unit-cell parameters vary smoothly but nonlinearly between 0 and 75 mole % Fe_2TiO_4. A relatively sharp break in the trend near $x = 0.75$ may be due to cation-deficient compositions in the most Fe_2TiO_4-rich specimens. Variation of the oxygen positional parameter with composition is similar to that of the cell parameter. However, the a vs. u trend reveals that a significant change in behavior takes place in the low-Ti region. These features may reflect the importance of cation-cation repulsive interactions and/or changes in Fe^{2+}–Fe^{3+} electron delocalization properties.

Diffuse scattering was observed in neutron diffraction patterns, its intensity increasing with increased Ti content. Some of this scattering may be influenced by short-range order, involving octahedral Fe–Ti and/or Fe^{2+}–Fe^{3+}. The apparently disordered Fe^{2+}–Fe^{3+} distribution inferred from magnetic data may pertain only to the average structure and might actually be a consequence of substantial cation ordering on a local scale. The present results provide no indication of whether or not a statistically-random Fe^{2+}–Fe^{3+} distribution is approached at high temperature for intermediate titanomagnetites. If so, then the Akimoto distribution may form on quenching and thus represent a low-temperature state rather than the high-temperature limit of cation disorder as has previously been supposed. Clearly, some type of high-temperature measurements, perhaps involving crystallographic, thermochemical, or electrical properties, will be required to resolve the actual cation distribution as a function of temperature.

Acknowledgments

Brookhaven National Laboratory provided use of its reactor and computing facilities. Lester Corliss, Julius Hastings, and Dave Cox (Brookhaven) are thanked for their assistance with neutron diffraction data collection and computations as well as for many enlightening discussions. The assistance of Pete Wasilewski (NASA Goddard) in collecting magnetic data is greatly appreciated. Discussions with and comments by Alexandra Navrotsky, Thomas Mason, Robert Von Dreele, and Michael Fleet were most helpful. Lois Koh is thanked for her art work. This research was supported in part by National Science Foundation Grants EAR76-22129 and EAR79-11285.

References

Akimoto, S. (1954) Thermomagnetic study of ferromagnetic minerals contained in igneous rocks. Journal of Geomagnetism and Geoelectricity, 6, 1–14.

Akimoto, S., Katsura, T., and Yoshida, M. (1957) Magnetic properties of $TiFe_2O_4$–Fe_3O_4 system and their change with oxidation. Journal of Geomagnetism and Geoelectricity, 9, 165–178.

Albee, A. L. and Ray, L. (1970) Correction factors for electron probe microanalysis of silicates, oxides, carbonates, phosphates, and sulfates. Analytical Chemistry, 42, 1408–1414.

Anderson, P. W. (1956) Ordering and antiferromagnetism in ferrites. Physical Review, 102, 1008–1013.

Aragón, R. and McCallister, R. H. (1982) Phase and point defect equilibria in the titanomagnetite solid solution. Physics and Chemistry of Minerals, 8, 112–120.

Banerjee, S. K., O'Reilly, W., Gibb, T. C., and Greenwood, N. N. (1966) Influence on hyperfine field of local variations in inverse spinels. Physics Letters, 20, 455–457.

Banerjee, S. K., O'Reilly, W., Gibb, T. C., and Greenwood, N. N. (1967) The behavior of ferrous ions in iron-titanium spinels. Journal of Physics and Chemistry of Solids, 28, 1323–1335.

Banerjee, S. K., O'Reilly, W., and Johnson, C. E. (1967) Mössbauer-effect measurements in FeTi spinels with local disorder. Journal of Applied Physics, 38, 1289–1290.

Barth, T. F. W. and Posnjak, E. (1932) Spinel structures: with and without variate atom equipoints. Zeitschrift für Kristallographie, A82, 325–341.

Bence, A. E. and Albee, A. L. (1968) Empirical correction factors for the electron microanalysis of silicates and oxides. Journal of Geology, 76, 382–403.

Bleil, U. (1971) Cation distribution in titanomagnetites. Zeitschrift für Geophysik, 37, 305–319.

Bleil, U. (1976) An experimental study of the titanomagnetite solid solution series. Pure and Applied Geophysics, 114, 165–175.

Bragg, W. H. (1915a) The structure of magnetite and the spinels. Nature, 95, 561.

Bragg, W. H. (1915b) The structure of the spinel group of crystals. Philosophical Magazine, 30, 305–315.

Buddington, A. F. and Lindsley, D. H. (1964) Iron-titanium oxide minerals and synthetic equivalents. Journal of Petrology, 5, 310–357.

Burns, R. G., Nolet, D. A., Parkin, K. M., McCammon, C. A., and Schwartz, K. B. (1980) Mixed-valence minerals of iron and titanium: correlations of structural, Mössbauer and electronic spectral data. In D.B. Brown, Ed., Mixed-Valence Compounds, p. 295–336. Reidel, Boston.

Chevallier, R., Bolfa, J., and Mathieu, S. (1955) Titanomagnétites et ilménites ferromagnétiques. (1) Etude optique, radiocristallographique, chimique. Bulletin de la Société Francaise de Minéralogie et de Cristallographie, 78, 307–346.

Claasen, A. A. (1926) The scattering power of oxygen and iron

for x-rays. Proceedings of the Physical Society (London), 38, 482–487.

DeBoer, F., van Santen, J. H., and Verwey, E. J. W. (1950) The electrostatic contribution to the lattice energy of some ordered spinels. Journal of Chemical Physics, 18, 1032–1034.

Deines, P., Nafziger, R. H., Ulmer, G. C., and Woermann, E. (1974) Temperature-oxygen fugacity tables for selected gas mixtures in the system C–H–O at one atmosphere total pressure. Bulletin of the Earth and Mineral Sciences Experiment Station, No. 88, Pennsylvania State University, University Park, Pennsylvania.

Delamoye, P. and Michel, A. (1969) Transformation cristallographique dans l'orthotitanate de magnésium. Comptes Rendus Hebdomadaires des Seances de L'Academie des Sciences, Series C: Sciences Chimiques, 269, 837–838.

Dickof, P. A., Schurer, P. J., and Morrish, A. H. (1980) Magnetic structure of zinc-substituted magnetite at 4.2 K. Physical Review, B22, 115–127.

Dieckmann, R. and Schmalzried, H. (1977) Defects and cation diffusion in magnetite (II). Berichte der Bunsen-Gesellschaft für physikalische Chemie, 81, 414–419.

Evans, B. J. (1973) Electrical conductivity and hyperfine interactions in $M_xFe_{3-x}O_4$ above and below T_N. American Institute of Physics Conference Proceedings, Magnetism and Magnetic Materials, 10, 1398–1402.

Evans, B. J. (1975) Experimental studies of the electrical conductivity and phase transition in Fe_3O_4. American Institute of Physics Conference Proceedings, Magnetism and Magnetic Materials, 24, 73–78.

Evans, B. J., Pan, L. S., and Vogel, R. H. (1976) Crystal chemistry and electron localization in Sn-doped Fe_3O_4. American Institute of Physics Conference Proceedings, Magnetism and Magnetic Materials, 29, 390–391.

Fleet, M. E. (1981) The structure of magnetite. Acta Crystallographica, B37, 917–920.

Fleet, M. E. (1982) The structure of magnetite: defect structure II. Acta Crystallographica, B38, 1718–1723.

Flood, H. and Hill, D. G. (1957) The redox equilibrium in iron oxide spinels and related systems. Berichte der Bunsen-Gesellschaft für physikalische Chemie, 61, 18–24.

Forster, R. H. and Hall, E. O. (1965) A neutron and x-ray diffraction study of ulvöspinel, Fe_2TiO_4. Acta Crystallographica, 18, 859–862.

Fujino, K. (1974) Cation distribution and local variation of site symmetry in solid solution series, Fe_3O_4–Fe_2TiO_4. Mineralogical Journal, 7, 472–488.

Gorter, E. W. (1957) Chemistry and magnetic properties of some ferrimagnetic oxides like those occurring in nature. Advances in Physics, 6, 336–361.

Haas, C. (1965) Phase transitions in crystals with the spinel structure. Journal of Physics and Chemistry of Solids, 26, 1225–1232.

Hamilton, W. C. (1958) Neutron diffraction investigation of the 119 K transition in magnetite. Physical Review, 110, 1050–1057.

Hargrove, R. S. and Kündig, W. (1970) Mössbauer measurements of magnetite below the Verwey transition. Solid State Communications, 8, 303–308.

Hewat, A. W. (1973) The Rietveld computer program for the profile refinement of neutron diffraction powder patterns modified for anisotropic thermal vibrations. U. K. Atomic Energy Research Establishment, Harwell, Report RRL 73/897.

Hill, R. J., Craig, J. R., and Gibbs, G. V. (1979) Systematics of the spinel structure type. Physics and Chemistry of Minerals, 4, 317–339.

Ishikawa, Y., Syono, Y., and Akimoto, S. (1964) Neutron diffraction study of Fe_3O_4–Fe_2TiO_4 series. Annual Progress Report, Rock Magnetism Research Group, Institute for Solid State Physics, University of Tokyo, Tokyo, 14–20.

Ishikawa, Y., Sato, S., and Syono, Y. (1971) Neutron and magnetic studies of a single crystal of Fe_2TiO_4. Technical Report of the Institute for Solid State Physics, University of Tokyo, Tokyo, Ser. A, No. 455.

Jacob, K. T. and Alcock, C. B. (1975) Evidence of residual entropy in the cubic spinel Zn_2TiO_4. High Temperatures–High Pressures, 7, 433–439.

Jensen, S. D. and Shive, P. N. (1973) Cation distribution in sintered titanomagnetites. Journal of Geophysical Research, 78, 8474–8480.

Katsura, T., Kitayama, K., Aoyagi, R., and Sasajima, S. (1976) High-temperature experiments related to Fe–Ti oxide minerals in volcanic rocks. In Kazan, Ed., Volcanoes, 21, 31–56.

Keefer, C. M. and Shive, P. N. (1981) Curie temperature and lattice constant reference contours for synthetic titanomaghemites. Journal of Geophysical Research, 86, 987–998.

Khattak, C. P. and Cox, D. E. (1977) Profile analysis of x-ray powder diffractometer data: structural refinement of $La_{0.75}Sr_{0.25}CrO_3$. Journal of Applied Crystallography, 10, 405–411.

Kündig, W. and Hargrove, R. S. (1969) Electron hopping in magnetite. Solid State Communications, 7, 223–227.

Lawson, C. (1978) Problems in the use of evacuated, sealed silica tubes for synthesis of single-phase compositions in the system FeO–Fe_2O_3–TiO_2. Carnegie Institution of Washington Year Book, 77, 917–922.

Lindsley, D. H. (1963) Fe–Ti oxides in rocks as thermometers and oxygen barometers. Carnegie Institution of Washington Year Book, 62, 60–66.

Lindsley, D. H. (1965) Iron–titanium oxides. Carnegie Institution of Washington Year Book, 64, 144–148.

Lindsley, D. H. (1978) Magnetite–ilmenite equilibria: solution models including MgO and MnO. (abstr.) EOS, 59, 395.

Mason, T. O. and Bowen, H. K. (1981) Electronic conduction and thermopower of magnetite and iron-aluminate spinels. Journal of the American Ceramic Society, 64, 237–242.

Moskowitz, B. M. and Banerjee, S. K. (1981) A comparison of the magnetic properties of synthetic titanomaghemites and some oceanic basalts. Journal of Geophysical Research, 86, 11869–11882.

Néel, L. (1948) Propriétés magnétiques des ferrites; ferrimagnétisme et antiferromagnétisme. Annales de Physique, 3, 137–198.

Néel, L. (1955) Some theoretical aspects of rock magnetism. Advances in Physics, 4, 191–243.

Newton, R. C. and Wood, B. J. (1980) Volume behavior of silicate solid solutions. American Mineralogist, 65, 733–745.

Nishikawa, S. (1915) The structure of some crystals of the spinel group. Proceedings of the Mathematical and Physical Society of Tokyo, 8, 199–209.

O'Donovan, J. B. and O'Reilly, W. (1980) The temperature dependent cation distribution in titanomagnetites: an experimental test. Physics and Chemistry of Minerals, 5, 235–243.

O'Reilly, W. and Banerjee, S. K. (1965) Cation distribution in titanomagnetites $(1\text{-}x)Fe_3O_4$–xFe_2TiO_4. Physics Letters, 17, 237–238.

Powell, R. and Powell, M. (1977) Geothermometry and oxygen barometry using coexisting iron-titanium oxides: a reappraisal. Mineralogical Magazine, 41, 257–263.

Prevot, M. and Poix, P. (1971) Un calcul du paramètre cristallin des titanomagnétites oxydées. Journal of Geomagnetism and Geoelectricity, 23, 255–265.

Prince, E. (1981) Comparison of profile and integrated-intensity methods in powder refinement. Journal of Applied Crystallography, 14, 157–159.

Readman, P. W. and O'Reilly, W. (1972) Magnetic properties of oxidized (cation deficient) titanomagnetites $(Fe,Ti\square)_3O_4$. Journal of Geomagnetism and Geoelectricity, 24, 69–90.

Rietveld, H. M. (1969) A profile refinement method for nuclear and magnetic structures. Journal of Applied Crystallography, 2, 65–71.

Riste, T. and Tenzer, L. (1961) A neutron diffraction study of the temperature variation of the spontaneous sublattice magnetization of ferrites and the Néel theory of ferrimagnetism. Journal of Physics and Chemistry of Solids, 19, 117–123.

Robbins, M., Wertheim, G. K., Sherwood, R. C., and Buchanan, D. N. E. (1971) Magnetic properties and site distributions in the system $FeCr_2O_4$–Fe_3O_4($Fe^{2+}Cr_{2-x}Fe^{3+}_xO_4$). Journal of Physics and Chemistry of Solids, 32, 717–729.

Rumble, D. (1970) Thermodynamic analysis of phase equilibria in the system Fe_2TiO_4–Fe_3O_4–TiO_2. Carnegie Institution of Washington Year Book, 69, 198–207.

Rumble, D. (1977) Configurational entropy of magnetite–ulvöspinel$_{ss}$ and hematite–ilmenite$_{ss}$. Carnegie Institution of Washington Year Book, 76, 581–584.

Sakata, M. and Cooper, M. J. (1980) An analysis of the Rietveld profile refinement method. Journal of Applied Crystallography, 12, 554–563.

Sato, M. (1971) Electrochemical measurements and control of oxygen fugacity and other gaseous fugacities with solid electrolyte sensors. In G. C. Ulmer, Ed., Research Techniques for High Pressure and High Temperature, p. 43–101. Springer-Verlag, New York.

Sawatzky, G. A. and van der Woude, F. (1974) Covalency effects in hyperfine interactions. Journal de Physique, 35, C6, 47–60.

Shannon, R. D. (1976) Revised effective ionic radii and systematic studies of interatomic distances in halides and chalcogenides. Acta Crystallographica, A32, 751–767.

Shirane, G. (1959) A note on the magnetic intensities of powder neutron diffraction. Acta Crystallographica, 12, 282–285.

Shull, C. G., Wollan, E. O., and Koehler, W. C. (1951) Neutron scattering and polarization by ferromagnetic materials. Physical Review, 84, 912–921.

Simons, B. and Woermann, E. (1978) Iron titanium oxides in equilibrium with metallic iron. Contributions to Mineralogy and Petrology, 66, 81–89.

Smit, J. and Wijn, H. P. J. (1959) Ferrites. Wiley, New York.

Spencer, K. and Lindsley, D. H. (1981) A solution model for coexisting iron–titanium oxides. American Mineralogist, 66, 1189–1201.

Stephenson, A. (1969) The temperature dependent cation distribution in titanomagnetites. Geophysical Journal of the Royal Astronomical Society, 18, 199–210.

Stephenson, A. (1972) Spontaneous magnetization curves and Curie points of spinels containing two types of magnetic ion. Philosophical Magazine, 25, 1213–1232.

Stout, M. Z. and Bayliss, P. (1975) Crystal structure of a natural titanomagnetite. Canadian Mineralogist, 13, 86–88.

Stout, M. Z. and Bayliss, P. (1980) Crystal structure of two ferrian ulvöspinels from British Columbia. Canadian Mineralogist, 18, 339–341.

Taylor, R. W. (1964) Phase equilibria in the system FeO–Fe_2O_3–TiO_2 at 1300°C. American Mineralogist, 49, 1016–1030.

Van der Woude, F., Sawatzky, G. A., and Morrish, A. H. (1968) Relation between the hyperfine magnetic fields and sublattice magnetizations in Fe_3O_4. Physical Review, 167, 533–535.

Vincent, H., Joubert, J.-C., and Durif, A. (1966) Etude structurale des formes ordonnées des orthotitanates de zinc et de manganèse. Bulletin de la Société Chimique de France, 246–250.

Wasilewski, P., Virgo, D., Ulmer, G. C., and Schwerer, F. C. (1975) Magnetochemical characterization of $Fe(Fe_xCr_{2-x})O_4$ spinels. Geochimica et Cosmochimica Acta, 39, 889–902.

Watson, R. E. and Freeman, A. J. (1961) Hartree–Fock atomic scattering factors for the iron transition series. Acta Crystallographica, 14, 27–37.

Webster, A. H. and Bright, N. F. H. (1961) The system iron–titanium–oxygen at 1200°C and oxygen partial pressures between 1 atmosphere and 2×10^{-14} atmosphere. American Ceramic Society Journal, 44, 110–116.

Wechsler, B. A. (1981) Crystallographic studies of titanomagnetites and ilmenite. Ph.D. Thesis, State University of New York, Stony Brook.

Wechsler, B. A. and Navrotsky, A. (1982) Thermochemistry of compounds in the system MgO–TiO_2. (abstr.) Geological Society of America Abstracts with Programs, 14, 643–644.

Wechsler, B. A. and Von Dreele, R. B. (1983) Structure refinement of high and low temperature Mg_2TiO_4 spinels from neutron powder diffraction data. (abstr.) American Crystallographic Association Program and Abstracts, 11, 33.

Williams, R. J. (1972) A solid ceramic electrolyte system for measuring redox conditions in high-temperature gas mixing studies. NASA Technical Memorandum TM X-58105.

Wu, C. C. and Mason, T. O. (1981) Thermopower measurement of cation distribution in magnetite. Journal of the American Ceramic Society, 64, 520–522.

Yakel, H. L. (1980) Determination of the cation site-occupation parameter in a cobalt ferrite from synchrotron-radiation diffraction data. Journal of Physics and Chemistry of Solids, 41, 1097–1104.

Manuscript received, June 28, 1982;
accepted for publication, January 18, 1984.